For proceedings of Sixth Hypervelocity Impact Symposium
Cleveland, Ohio, April 30, May 1-2, 1963

38 p.

THE PARTITION OF ENERGY FOR HYPERVELOCITY IMPACT CRATERS FORMED IN ROCK

By Donald E. Gault and Ezra D. Heitowit

National Aeronautics and Space Administration
Ames Research Center
Moffett Field, Calif.

N65-88736

[redacted]

ABSTRACT

14932

An analysis is presented of the manner in which energy was expended from the original reservoir of projectile kinetic energy during the formation of impact craters in rock. The study is based on an extensive series of cratering experiments employing aluminum projectiles launched with a nominal velocity of 6.25 km/sec against blocks of macroscopically homogeneous basalt. It is shown that a major fraction of the projectile kinetic energy reappears in kinetic form in the ejecta spewed out of the craters. Significant, but smaller, fractions of energy are trapped irreversibly as heat in the rock and projectile material and expended in the creation of free surfaces by fragmentation.

THE PARTITION OF ENERGY FOR HYPERVELOCITY
IMPACT CRATERS FORMED IN ROCK

By Donald E. Gault and Ezra D. Heitowit

National Aeronautics and Space Administration
Ames Research Center
Moffett Field, Calif.

INTRODUCTION

The collision of a large meteoroid with the lunar or terrestrial surface is one of the ultimate examples of hypervelocity impact in the solar system. On a time scale measured in minutes, large geological structures can be produced, even for what corresponds to a relatively modest event. A terrestrial example of a planetary impact is the 1.2 km diameter crater at Meteor Crater, Arizona, but many others, including the Holleford (2.3 km), Brent (3.5 km), Deep Bay (12 km) Craters, the Ries Basin (27 km), Germany, and the Vredefort Ring (60 km), South Africa, have been interpreted as impact features (refs. 1 - 4). From dimensional considerations alone, these and countless similar lunar structures illustrate the violence of a cosmic impact and attest that the energy expenditures for formation of the craters may dwarf by orders of magnitude the energy released by the largest nuclear explosions.

Because of the obvious manifestations of the violence of such events, including evidence for fusion of the meteorite and country rock, as well as structural similarities to chemical and nuclear explosion craters, a remarkably persistent concept has been perpetuated that meteorite craters are produced by explosion of the meteorite body and rock heated by the collision. This concept has been so widely disseminated that any craters formed by hypervelocity impact are commonly referred to as explosion craters. The logic for this belief stems from a simple computation in which the specific kinetic energy of the projectile is equated to the specific internal energy of the projectile at the moment of impact. For impact velocities in excess of approximately 4.5 km/sec, a velocity well below the usual geocentric velocity of large meteoroids, it is easily found that the specific internal energies thus calculated exceed the enthalpy of vaporization for any solid at atmospheric pressures. The obvious, although incorrect, conclusion is that the heated mass of projectile explodes.

The principal fallacy in such a calculation (first pointed out, to the authors' knowledge, by Shoemaker (ref. 1)) is in the neglect of the manner in which energy is partitioned in the projectile and target by shock processes. Moreover, the simple computation totally ignores the equation of state of the materials under shocked conditions. Hypervelocity impact can, in fact, produce very high specific internal energies. These energies are, however, the consequences of the mechanical compression by the projectile as it penetrates the target, rather than the cause of the compression. Moreover, when one considers the equation of state of the materials involved, only a fraction of the increase in specific internal energy is found to be irreversibly trapped as heat for fusion and/or vaporization. The remaining fraction of the internal energy is used in furthering the propagation of the shock waves through the media. In effect, any energy expended in fusing or vaporizing target or projectile material is lost to the cratering process and detracts from any physical enlargement of an impact crater. An impact, accompanied by vaporization, is an explosion only to the extent that debris is thrown upward and out of a transient cavity.

The energy partition described by Shoemaker is valid only during the earliest stages of energy transfer from projectile to target and provides no information on the ultimate deposition of the kinetic energy from the projectile at the conclusion of the cratering process. Notwithstanding this limitation, the significance of the analysis as related to "explosive" cratering is evident and it emphasizes that energy partition during a cratering event is one of the most interesting and fundamental problems which confront experimentalists and theorists in the field of hypervelocity impact.

Of the three quantities - mass, momentum, and energy - which are necessary to describe the motion of one body relative to another body, energy is by far the most difficult to trace through any complicated physical process. For this reason, there is very little hope for either formulating a theoretical model for impact cratering or interpreting experimental results with any insight into the physical processes of the phenomena, until a thorough understanding is obtained of the various paths into which the projectile kinetic energy is channeled during the formation of a crater.

As part of a general study at the Ames Research Center of the mechanics of hypervelocity impact and role of collision processes as an evolutionary factor in the solar system, it is the purpose of this paper to present results of an analysis which has been made to explore the manner in which energy is partitioned during the formation of impact craters in rock. The analysis is an outgrowth of earlier work reported by Moore, et al. (ref. 5) at the 5th Hypervelocity Impact Symposium, and by Gault, et al. (ref. 6) in relation to environmental factors of lunar impacts. The analysis is based on an extensive series of cratering experiments employing aluminum projectiles launched with a nominal velocity of 6.25 km/sec against blocks of macroscopically homogeneous basalt. The study makes use of high-speed framing records (5×10^3, 1.5×10^5 and 10^6 frames/sec) of impact events, mass size distributions of the fragmented rock ejecta, spallation of the back of the target blocks, ballistic pendulum measurements, and Hugoniot equations of state for aluminum and basalt.

ANALYSIS

Preliminary Consideration

A review of the initial energy transfer from projectile to target will be helpful to the subsequent discussion of the manner in which energy is partitioned during crater formation in rock. An exact treatment of the early stages of impacts is, of course, not possible at the present time, but an acceptable approximate solution can be obtained based on the hypothetical case of two semi-infinite bodies colliding along a plane surface. That is, the initial stage of the impact is considered as a problem in one-dimensional flow, a problem which is tractable mathematically and, at the same time, amenable to gaining some insight into early stages of the energy partition.

Initial Partition of Energy

With reference to the accompanying sketch, upon contact of the projectile against the target, shock waves will be propagated from the interface into both of the colliding bodies. Both shock waves will engulf a continuously increasing mass of material as the undisturbed

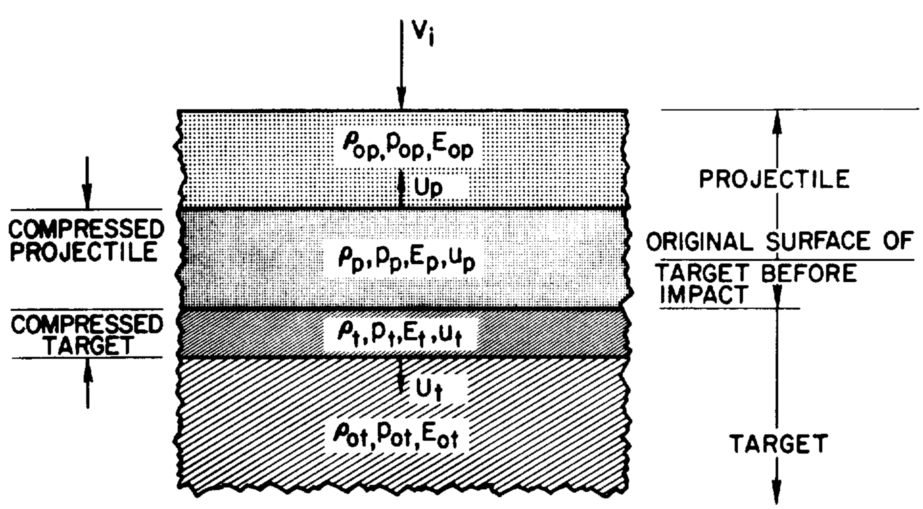

Sketch (a)

$$p_p = p_t \tag{1}$$

projectile continues to advance toward the target with the impact velocity V_i. In a coordinate system referenced to the undisturbed media, application of the laws of conservation of mass, momentum, and energy across the shocks leads to the well-known Rankine-Hugoniot equations

$$\rho_o U = \rho(U - u) \tag{2}$$

$$p - p_o = \rho_o U u \tag{3}$$

$$E - E_o = \frac{1}{2}(p + p_o)\left(\frac{1}{\rho_o} - \frac{1}{\rho}\right) = \frac{1}{2}u^2 \tag{4}$$

where U is the propagation velocity of the shock wave into the undisturbed medium, u is the mass velocity of the compressed material behind the shock wave, again relative to the undisturbed material, and p, ρ, and E are the pressure, density, and specific internal energy, respectively, with the subscript o denoting conditions in the undisturbed medium.

For conditions during a hypervelocity impact, $p \gg p_o$ and the last two expressions are frequently approximated as

$$p = \rho_o U u \tag{3a}$$

$$E - E_o = \frac{1}{2}p\left(\frac{1}{\rho_o} - \frac{1}{\rho}\right) = \frac{1}{2}u^2 \tag{4a}$$

It is to be noted that to the same degree of approximation, the total work done on the medium by the shock compression is $p(1/\rho_o - 1/\rho)$. Thus equation (4a) indicates that the energy added by the shock process is equally partitioned in the compressed material between the specific kinetic energy $(1/2\ u^2)$ and an increase in the specific internal energy $(E - E_o)$.

Since the density ρ_o may be considered a known quantity, the Rankine-Hugoniot equations provide three equations with four unknowns, ρ, p, U, and u. In order to fully describe the conditions behind the shock front, a fourth equation is required. Any algebraic equation involving two of the four unknowns would be satisfactory, but what is required in principle is a relationship which describes the thermodynamic properties of the material, that is, an equation of state.

The equation of state of solids has received increasing attention in recent years by workers in the field of solid-state physics. A discussion of this important subject is beyond the scope of this study and it is sufficient to note here only that a wealth of information on the subject has accumulated in the open literature. Most of the available data is concerned with metals, a wide selection up to pressures of a few megabars[1] (refs. 7 - 9) and a few metals for pressures approaching 10 megabars (ref. 10). Data for rocks and minerals are relatively scarce and confined to pressures less than 700 kilobars (ref. 11). For the present analysis for the impact of aluminum into basalt, the data of Walsh, et al. (ref. 8) and Al'tshuler, et al. (ref. 9) will be used for the aluminum and the data of Lombard (ref. 11) for a basalt from the Nevada Test Site will be employed for the target medium.

The usual manner of presenting the equation of state under shock conditions is the so-called Hugoniot curve describing the locus of points for the specific volume ($v = 1/\rho$) to which a material is compressed by any given pressure jump across the shock front. The appropriate Hugoniot curves for Al and basalt are shown in figure 1. The two materials have similar Hugoniots with the Al being stiffer in the sense that the percentage change in the volume for a given pressure is less than that for the basalt. It must be emphasized that the Hugoniot curves themselves do not indicate a continuous compression cycle to a pressure p; the curves are only the locus of points for the states attained by discontinuous pressure jumps.

The experimental Hugoniot curves (fig. 1), together with equations (2), (3a), and (4a), permit the evaluation of U, u, p, $E - E_0$, and ρ in terms of each other for any given conditions. The application of these data, however, would be cumbersome if it were not for the fortuitous result that an "equation of state" expression can be given algebraically in terms of the shock wave and mass velocities U and u. It has been found that an excellent approximation for the experimental results over a wide range of pressure can be made by an expression in the form

$$U = a + bu \tag{5}$$

where a and b are constants. Departures from this linear relationship are usually associated with phase changes and/or high dynamic yield strengths, both of which may lead to conditions for which a single shock system is unstable and breaks down into a system of two or more compression waves (ref. 12). The graphical representation of the equations for aluminum and basalt is shown in figure 2, with the numerical forms used herein being

$$U_p = 5.30 + 1.37\, u_p \tag{6}$$

---

[1]One bar = 10^6 dynes/cm^2 (i.e., approximately 1 atmosphere).

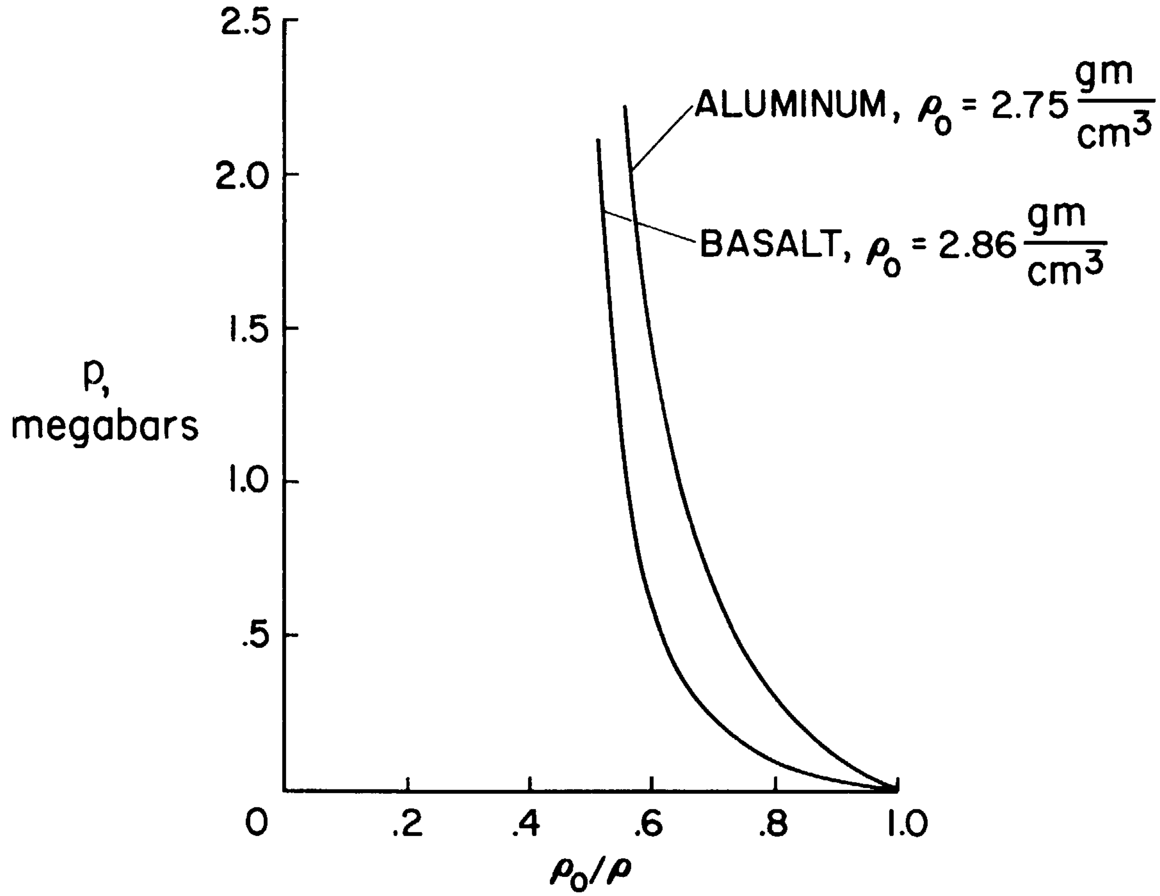

Figure 1.- Hugoniot curves for aluminum and basalt.

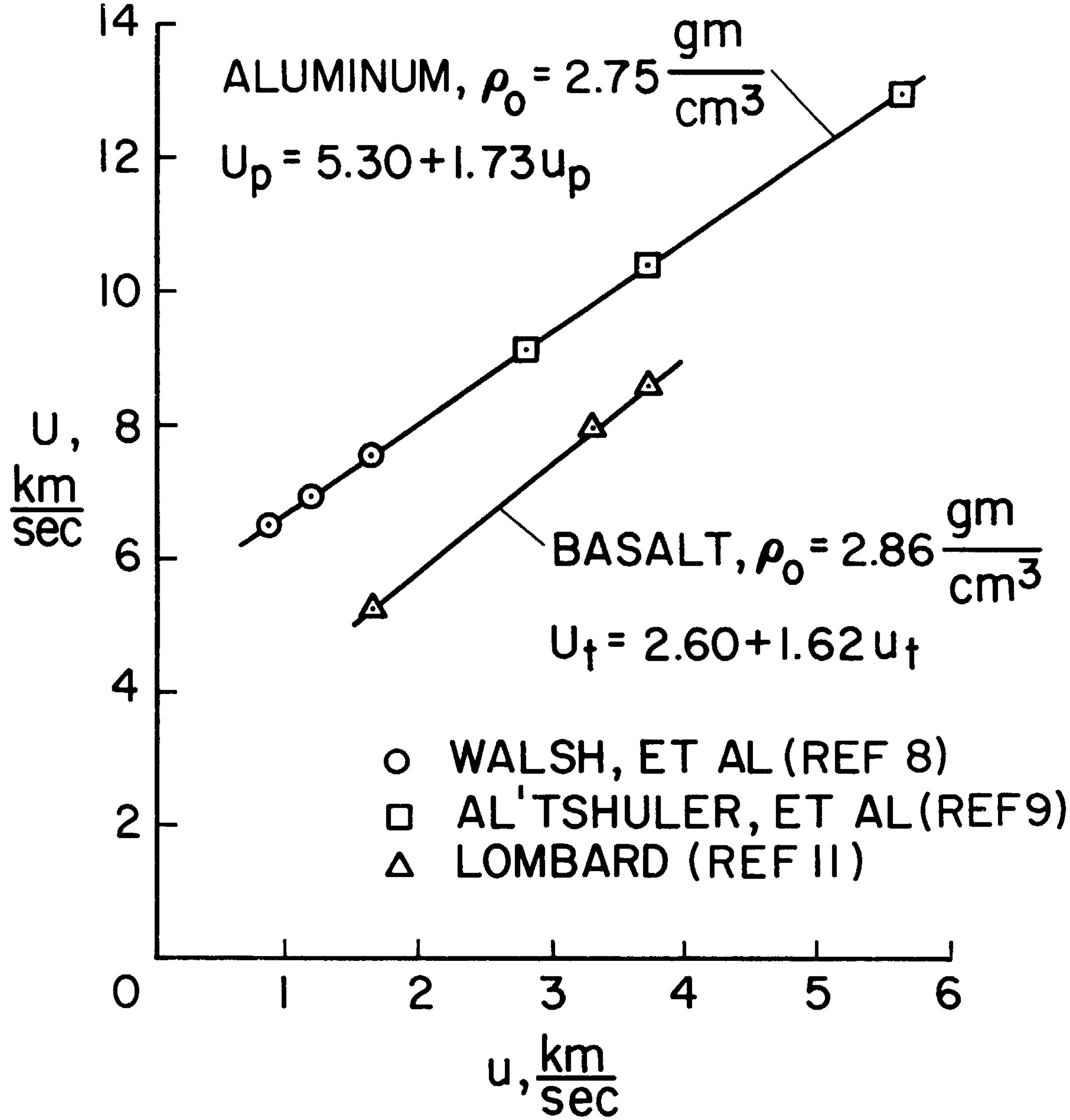

Figure 2.- Shock-wave and mass velocity relationship for aluminum and basalt.

NATIONAL AERONAUTICS AND SPACE ADMINISTRATION
AMES RESEARCH CENTER, MOFFETT FIELD, CALIFORNIA

for the aluminum projectile and

$$U_t = 2.60 + 1.62\, u_t \tag{7}$$

for the basalt target.

Although equations (6) and (7), when combined with equations (2), (3a), and (4a), provide a simple algebraic solution for U, u, p, ρ, and $E - E_o$ in terms of each other for any given conditions, it remains to relate the conditions behind the wave fronts to the impact velocity V_i. Toward this end, with the aid of sketch (a), it is readily verified that since the compressed projectile must have the same relative velocity to the undisturbed target $(V_i - u_p)$ as the velocity of the compressed target medium (U_t) to maintain physical contact at the projectile-target interface, there results

$$V_i = u_p + u_t \tag{8}$$

When the shock velocity U is eliminated between equations (3a) and (5), so that

$$p = \rho_o(a + bu)u \tag{9}$$

and equation (8) is employed to eliminate u_p (or u_t), one may write

$$p_p = \rho_{op}[a_p + b_p(V_i - u_t)](V_i - u_t) \tag{10}$$

$$p_t = \rho_{ot}(a_t + b_t u_t)u_t \tag{11}$$

Then, because the pressure in the shocked target and projectile media must be equal, a simple quadratic in V_i and u_t (or u_p) results

$$[a_p + b_p(V_i - u_t)](V_i - u_t) = \rho_{ot}(a_t + b_t u_t)u_t \tag{12}$$

which, in principle, permits an exact algebraic solution for all the required parameters as a function of the impact velocity V_i. In practice, however, a simple graphical solution can be obtained which is more in keeping with the spirit of the approximate analysis of the initial energy partition for the impact based on one-dimensional flow. When one notes that the pressure p can be calculated as a function of the mass velocity u from equation (9), equation (8) suggests the question, "At what pressure p will the sum of the mass velocities u_t and u_p (measured with respect to the undisturbed materials) equal a given value of the impact velocity V_i?" The graphical solution to this question is indicated in figure 3, together with the variation of p with V_i for the particular case under consideration of aluminum into basalt.[2] For the nominal impact velocity of 6.25 km/sec in this analysis, the pressure at impact is found to be 750 kilobars with $u_t = 3.30$ km/sec and $u_p = 2.35$ km/sec. The remaining parameters are easily determined from equations (6), (7), (2), (3a), and (4a).

$$U_t = 7.95 \text{ km/sec}$$

$$U_p = 9.34 \text{ km/sec}$$

$$E_t - E_{to} = 1/2\ U_t^2 = 5.45\times10^{10} \text{ erg/g}$$

$$E_p - E_{po} = 1/2\ U_p^2 = 4.35\times10^{10} \text{ erg/g}$$

$$\rho_t/\rho_{ot} = 1.71$$

$$\rho_p/\rho_{op} = 1.46$$

It is now possible to ascertain the initial partition of energy between projectile and target within, of course, the limitations of the one-dimensional analysis. At the instant the entire projectile becomes engulfed by the shock compression over the length (diameter) d, the interface between target and projectile will have advanced a distance $(u_t/U_p)d = 0.353d$ into the target and the shock front in the target will have advanced a distance $(U_t/U_p)d = 0.851d$ from the face of the target. The total mass of the engulfed projectile will be $\rho_{op}d = 2.75d$ g/cm^2, while $\rho_{ot}(U_t/U_p)d = 2.44d$ g/cm^2 of target material will be consumed by the shock compression. The increase in internal energy for the projectile is $1/2\rho_{op}u_p{}^2d = 1.2d\times10^{11}$ erg/cm^2 and for the target $1/2\rho_{ot}(U_t/U_p)u_t{}^2d = 1.33d\times10^{11}$ erg/cm^2. The kinetic energy in the compressed target medium will also be $1.33d\times10^{11}$ erg/cm^2, while the residual kinetic energy in the projectile, traveling at a velocity u_t relative to the undisturbed target will be $1/2\rho_{op}u_t{}^2 = 1.5d\times10^{11}$ erg/cm^2. A summation of these energies gives $1/2\rho_{op}V_i{}^2d = 5.36d\times10^{11}$ erg/cm^2, the kinetic energy of the original undisturbed projectile material.

---

[2]The NTS basalt has a density of $\rho_o = 2.68$ g/cm^3. The basalt employed in the experiments has a density of 2.86 g/cm^3; the latter value has been used in the calculations.

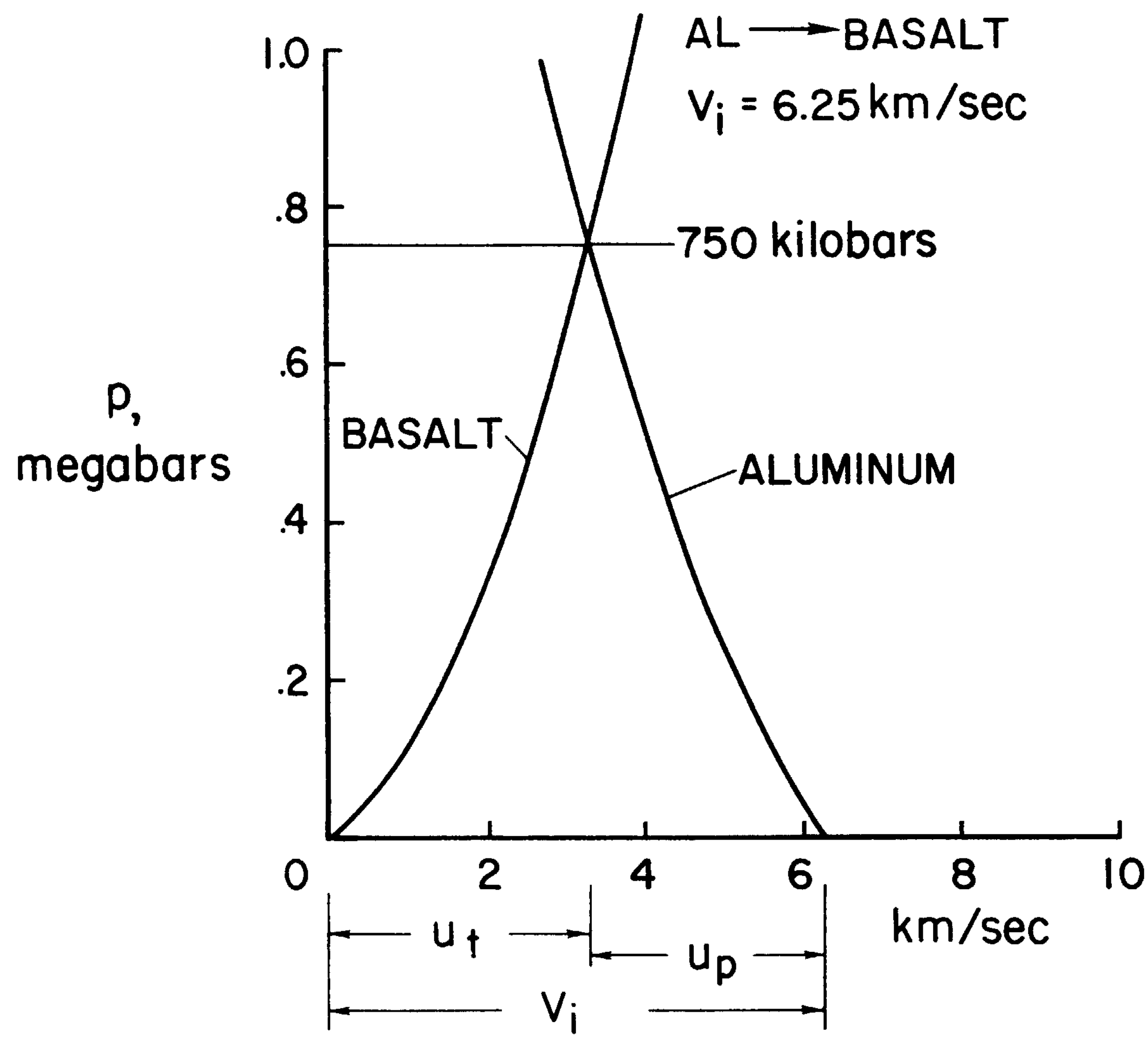

Figure 3.- Graphical solution for determining pressure and mass velocities for one-dimensional impact of dissimilar materials.

NATIONAL AERONAUTICS AND SPACE ADMINISTRATION
AMES RESEARCH CENTER, MOFFETT FIELD, CALIFORNIA

A summary of the initial partition of energy for the Al into basalt at 6.25 km/sec is given in the following table:

	Energy	Percent of original projectile kinetic energy	
Projectile	Internal, $E_p - E_{po}$	22.3	50.2
	Kinetic, $1/2\rho_p u_t^2$	27.9	
Target	Internal, $E_t - E_{to}$	24.9	49.8
	Kinetic, $1/2\rho_t u_t^2$	24.9	

It should be noted that general algebraic expressions for the initial energy partition can be given if the energy retained by the projectile is considered to be (in normalized form)

$$\frac{\text{Energy retained by projectile}}{1/2\rho_{op}V_i^2} = \frac{u_p^2 + u_t^2}{(u_p + u_t)^2} = \frac{1 + (u_p/u_t)^2}{(1 + u_p/u_t)^2} \qquad (13)$$

so that the fraction of the original projectile kinetic energy delivered to the target becomes

$$\frac{\text{Energy delivered to target}}{1/2\rho_{op}V_i^2} = \frac{2u_p/u_t}{(1 + u_p/u_t)^2} \qquad (14)$$

Although the energy delivered to the target is equally split between the increase in internal energy and the kinetic energy of the compressed mass behind the shock front, the energy retained by the projectile is composed of residual kinetic energy,

$$\frac{\text{Residual projectile kinetic energy}}{1/2\rho_{op}V_i^2} = \frac{1}{(1 + u_p/u_t)^2} \qquad (15)$$

and the increase in internal energy

$$\frac{\text{Projectile internal energy}}{1/2\rho_{op}V_i^2} = \left(\frac{u_p/u_t}{1 + u_p/u_t}\right)^2 \qquad (16)$$

Equations (13) and (14) clearly indicate that, except for the special case involving impacts of similar materials for which $u_p = u_t = 1/2V_i$ (see eq. (12)), the energy retained by the projectile will never be equal to that transferred to the target. For the particular case in which the projectile density is much greater than the target density, say Fe into the basalt, u_t becomes large compared to u_p and the fraction of energy transferred to the target becomes relatively smaller (eq. (14)). Moreover, within the projectile, the increase in internal energy becomes less and most of the original kinetic energy is retained in kinetic form by the compressed projectile material. Results similar to the previous tabulation for Fe into basalt at 6.25 km/sec are tabulated below:

	Energy	Percent of original projectile kinetic energy	
Projectile	Internal, $E_p - E_{op}$	10.5	56.2
	Kinetic, $1/2\rho_p u_t^2$	45.7	
Target	Internal, $E_t - E_{ot}$	21.9	43.8
	Kinetic, $1/2\rho_t u_t^2$	21.9	

For these calculations $U_p = 3.75 + 1.66u_p$ (ref. 9) and $\rho_o = 7.85$ g/km^3.

The summary tabulations and equations (13) through (16) demonstrate just one of the errors in equating projectile kinetic energy to specific internal energy in the projectile material for an "explosive" impact.

Irreversible Heating

The conditions following the initial partition of energy for an impact are roughly analogous to those occurring after an abrupt removal of a steady force which has bodily accelerated and compressed a simple coil spring along its longitudinal axis. Once the external accelerating force has been removed from the spring, the internal forces produced by the stresses set up in the compressed coils are unopposed and will cause the spring to expand back to its original length. In the somewhat analogous situation, once the projectile is totally engulfed by the shock wave racing out from the projectile-target interface, the internal forces arising from the compressive stresses in the shocked material are unopposed at the free surface of the back of the projectile and will cause the compressed mass to expand. The expansion is accomplished by pressure release (i.e., rarefaction) waves which propagate back into the shocked material and relieve the stresses to zero.

The expansions for both the spring and impact, of course, are capable of doing useful work. It is to be noted that for the particular case of an impact, any internal energy expended as useful work during the expansion of the compressed mass reduces the energy which can be ultimately deposited thermally at the zero pressure state. This point can be illustrated with the aid of the accompanying sketch. The sketch shows schematically a Hugoniot curve and a pressure release curve for an isentropic ($dS = 0$)

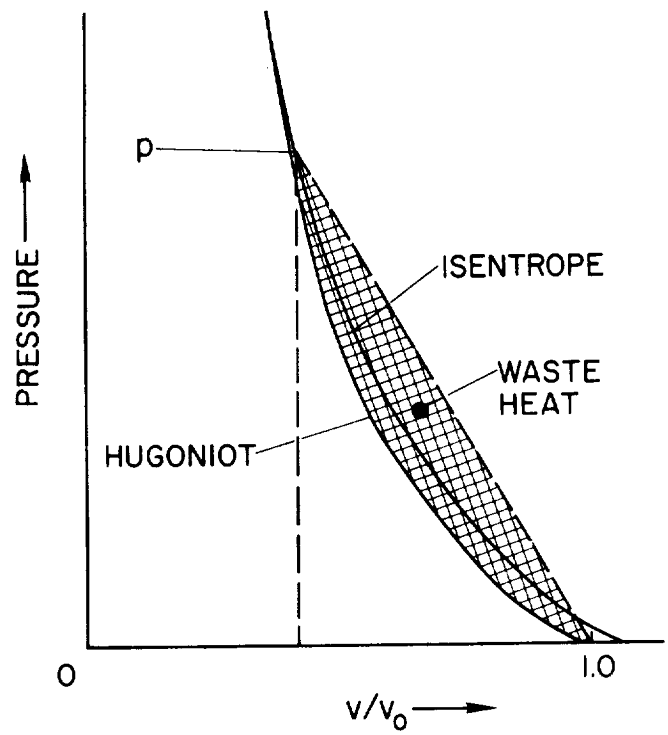

Sketch (b)

rarefaction wave relieving the pressure from p_1 to zero. In contrast to the Hugoniot, the isentrope describes a continuous process. The useful work done by the expansion, therefore, is represented by the cross-hatched area below the isentrope. Since the shock compression increases the internal energy by an amount equivalent to the triangular area indicated by the dashed lines, there is effectively a "hysteresis loop" in the compression-release cycle for the target and projectile materials which contribute energy for irreversible heating of the shocked media. Thus, not only is the increase in internal energy in, say, the projectile, a fraction of the original projectile kinetic energy (as previously discussed), but only a fraction of the fractional increase is ever made available for fusing and/or vaporizing target and projectile material. The concept of "explosive" impact totally ignores both the initial partition of energy and the energy returned as useful work during the expansion of the shock compressed mass.

For the present analysis of the impact of Al into basalt, the one-dimensional model from the previous section provides a convenient basis for estimating the energy deposited irreversibly as heat in the projectile. Under the assumption of one-dimensional flow and having a complete p, v, E, s equation of state, it has been shown by Rice, et al. (ref. 12) that the pressure p_a along any adiabatic release curve can be obtained from the integration of the linear first-order differential equation

$$\frac{dp_a}{d\overline{v}} + \frac{\gamma}{\overline{v}}\left[1 + \frac{d}{d\overline{v}}\left(\frac{\overline{v}}{\gamma}\right)\right] p_a = \frac{dp_h}{d\overline{v}} + p_h\left(\frac{\gamma}{\overline{v}}\right)\frac{d}{d\overline{v}}\left(\frac{\overline{v}}{\gamma}\right) - \frac{\gamma}{\overline{v}}\frac{dE_h}{d\overline{v}}\rho_o$$

Here, the subscripts a and h denote conditions on, respectively, the pressure release and Hugoniot curves with $\gamma = \gamma(\overline{v})$ the Grüneisen ratio and $\overline{v} = \rho_o/\rho$ the ratio of specific volumes. Rice, et al. (ref. 12) and Walsh and Christian (ref. 8) have presented results for 24ST aluminum for expansion from 513 kbars and 350 kbars, respectively. Additional calculations have been carried out by the authors for other pressures. Once $p_a = p_a(\overline{v})$ is known, the pv work done by the expansion to zero pressure is easily calculated, and the residual internal energy irreversibly trapped in the projectile, ΔE_p, is found from

$$\Delta E_p = \frac{1}{2} u_p^2 - (\text{pv work})$$

The results for ΔE_p normalized with respect to the original increase in internal energy, $E_p - E_{po} = 1/2\ u_p^2$, are shown in figure 4 as a function of the impact velocity, V_i. For the impact velocity of 6.25 km/sec, 8.2×10^9 erg/g, or only 19 percent of the increase in the projectile specific internal energy, is expended for irreversible heating. This corresponds to only 4 percent of the original projectile kinetic energy.

With a mean value for the specific heat of 10^7 erg/g/°C, sufficient energy, however, is deposited as heat to partially melt the projectile. Incipient melting in Al occurs at a temperature of approximately 660° C, a temperature that requires 6.4×10^9 erg/g starting from a nominal room temperature of 20° C. Approximately 1.8×10^9 erg/g is, therefore, available for fusion. Since the heat of fusion for Al is 3.9×10^9 erg/g, the impact should fuse approximately one-half (0.46) of the projectile mass.

Although this analysis illustrates the error in equating projectile kinetic energy to an increase in the specific internal energy of the projectile, the numerical results must be considered only an approximation based on the one-dimensional flow model. Two additional important factors must be considered. For a projectile with finite dimensions, rarefaction waves will eat in from the surfaces at the lateral boundaries of the projectile. These waves will act to attenuate the intensity of the shock

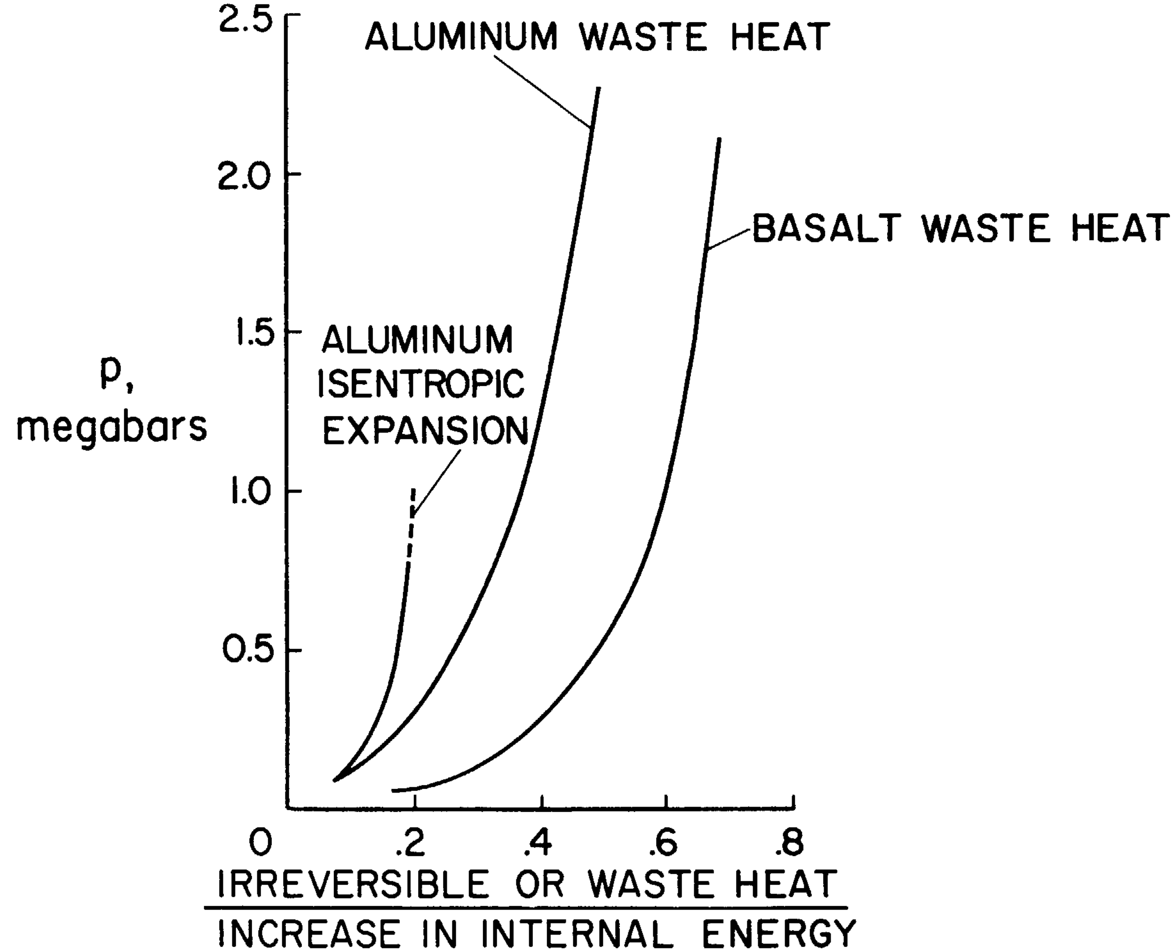

Figure 4.- The variation of irreversible and waste heat with pressure.

compression and, at the same time, strong pressure gradients within the projectile will cause material to flow laterally away from the point of impact. It is this lateral flow which effectively turns the projectile "inside out" and plates the projectile material on the interior of the embryonic crater (ref. 13). The reduction in the intensity of the shock pressures, of course, will tend to reduce the energy ultimately converted to heat. On the other hand, considerable energy will be expended in doing work against the viscous forces arising within the semiplastic or fluid mass flowing laterally toward the free surfaces of the projectile.

Evidence for the significance of shear stresses as a means of expending energy has been presented by Moore, et al. (ref. 14) for the case of a steel projectile impacting (4.25 km/sec) Coconino sandstone obtained from the site of the Arizona meteor crater. Less than 5 percent of the energy required to fuse the projectile could have been supplied by the shock compression, yet approximately 10 percent of the projectile mass (most of which was recovered in the ejecta) was obviously melted as a result of the impact. The total energy expended as heat in the steel projectile, therefore, must have been at least two to three times greater than the energy calculated from one-dimensional shock theory.

Similar effects unquestionably would occur as the result of the Al impact in basalt at 6.25 km/sec, but there is, unfortunately, no simple basis upon which to estimate the over-all results. In the absence of a more rigorous means for taking into account the counterbalancing effects of the rarefaction waves and the viscous dissipation of energy, the factor of 3 indicated by the experimental results for the steel into Coconino sandstone will be arbitrarily invoked for establishing an upper limit for the energy trapped as heat in the aluminum. By this means, it is suggested that perhaps as much as 60 percent of the increase in the specific internal energy in the aluminum was trapped as heat. This increase in energy would be adequate to fuse the entire projectile and vaporize approximately 14 percent of the projectile mass. Such a result is consistent with both optical and electron microscopic examination of the ejecta recovered from the impacts. No fragments of the projectile could be identified in the ejecta recovered from the impacts at 6.25 km/sec. Ample evidence for melting was present, however, in the form of submicron spherules, the shape only a true liquid would assume under the action of surface tension.

Turning now to the target, the calculation of the irreversible heating is beset with two problems. The first and most serious problem is the lack of a thermodynamic equation of state for the basalt, or, in fact, for any rock. Specifically, without some knowledge of the decompression isentropes which depend on a complete thermodynamic description of the material, it is impossible to calculate either the internal energy which can be recovered as useful work, or the energy which would be spend as irreversible heat.

To circumvent this lack of a thermodynamic description of the basalt equation of state, the concept of "waste heat" will be employed as a means for estimating the irreversible heating of the target medium (ref. 15). In so doing, the Hugoniot curve is taken as an approximation for the expansion isentrope (see sketch (b)).

With the Hugoniot curve approximation for the expansion isentrope after a material is shocked to a pressure p, it can be shown that the energy for irreversible heating (waste heat) can be expressed

$$\Delta E_t = \frac{1}{2} u^2 \left\{ 1 - 2 \left[\frac{a}{bu} + \left(\frac{a}{bu} \right)^2 \log \left(\frac{a}{a + bu} \right) \right] \right\} \tag{17}$$

where the relationship given as equation (11) can be used to express $u = u(p)$. An alternative form which will be useful later in the discussion is

$$\Delta E_t = \frac{1}{\rho_o} \frac{1}{2} p\eta - \left(\frac{a}{b} \right)^2 \left[\frac{b\eta}{1 - b\eta} + \log(1 - b\eta) \right] \tag{18}$$

with

$$\eta = 1 - \frac{v}{v_o} = 1 - \frac{\rho_o}{\rho}$$

Results for the basalt are shown in figure 4. Although this procedure will overestimate the energy trapped irreversibly in a metal (as shown in fig. 4 for the aluminum) the overestimation is only a factor of 2 and, in effect, will probably account for the additional energy spent against viscous forces as previously discussed. The "waste heat" approximation is probably most valid for rocks, however, and particularly for porous media such as pumice, tuff, sand, and sandstone. These latter materials, because of the intergranular pore spaces, return after the compression-release cycle to a higher density than their original unshocked values.

In contrast to the projectile for which a given mass is shocked to a nominal pressure and then decompressed, only a small fraction of the target mass which is engulfed by shock attains the nominal pressure calculated from the one-dimensional model. The radial propagation of the shock away from the point of impact into the target will tend to smear the energy of the impact through a progressively increasing mass of target material. Since the total energy within the shock system must remain constant (or decrease as the result of ejecta thrown out of the transient cavity), the specific energy behind the shock must decrease as the wave engulfs more and more mass. The shock pressures, therefore, must decrease with increasing distance from the point of impact and the heat deposited irreversibly at any point in the target becomes a function of the distance from the point of impact. An estimate for the irreversible heating of the target, therefore, depends on the pressure decay and, interdependently, the pressure decay depends on the consumption of the available energy by the irreversible heating.

It will be instructive at this point to neglect the irreversible heating at first and consider two simplified cases for the pressure decay.

Toward this end, reference is made to an adaptation of the Charters and Summers (ref. 16) ballistic model of cratering, as illustrated in the sketch. Here the shock front, assumed hemispherical in form, has propagated outward from the point of impact a distance r_2 into the target

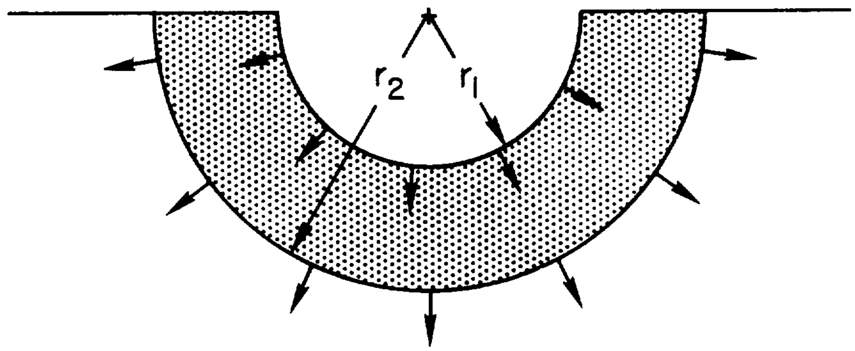

Sketch (c)

medium. The radius of the transient cavity is r_1 and the mass in the hemispherical shell of thickness $(r_2 - r_1)$ is

$$\frac{2}{3}\pi\rho_o r_2^3$$

For simplicity and following Charters and Summers, the pressure or stress is assumed constant within the shell of compressed material. Then, if the energy delivered to the target is E_t and this energy is uniformly distributed throughout the compressed mass behind the shock front, one can write

$$E_t = \rho_o \frac{2}{3}\pi r_2^3 p(v_o - v) = \frac{2}{3}\pi r_2^3 p\eta \tag{19}$$

where $p(v_o - v)$ is the specific energy added to the mass $\rho_o(2/3)\pi r^3$ by the shock compression to a pressure p. For the special case in which the Hugoniot is linear

$$p = c\eta$$

with c equal to a constant, the total energy becomes

$$E_t = \frac{2}{3}\pi r_2^3 \frac{p^2}{c} \tag{20}$$

so that

$$p \sim r^{-3/2} \tag{21}$$

When an experimental Hugoniot is inserted in equation (19)

$$E_t = \rho_o \frac{\pi}{3} r_2{}^3 \left[\frac{2p}{\rho_o b} + \left(\frac{a}{b}\right)^2 - \frac{a}{b}\sqrt{\frac{a^2}{b} + \frac{4p}{\rho_o b}}\;\right] \tag{22}$$

and one finds that for high pressures, say $p > 1$ mbar, the pressure variation tends to

$$p \sim r^{-3} \tag{23}$$

while in the lower range, $p > 100$ kbar, the pressure variation with r tends toward the inverse 3/2 relationship. In both cases (eqs. (21) and (23)) the length of the wave, that is, the distance $(r_2 - r_1)$, would increase as the pressure decreases in accordance with physical reality, but the model is obviously an oversimplification of the actual cratering process, since rarefaction waves would preclude maintaining the entire shell at a pressure p. Nevertheless, the model is useful in showing how the spherical divergence of the shock front produces a rapid decay in the pressure with distance from the point of impact. Ultimately, of course, the front decays into simple elastic waves and it is to be noted that Rinehart (ref. 17) has shown that for an elastic wave of constant length, velocity, and shape, the pressure decays inversely with the first power of the radial distance.

It should be expected that incorporating the effects of irreversible heating in the model should accelerate the decay of the pressures relative to the preceding examples, particularly at the higher pressures for which the irreversible heating becomes a major fraction of the increase in internal energy. This can be shown rather easily if one considers that as the shock front engulfs a differential mass

$$\rho_o \pi r^2 \, dr$$

energy is deposited in the differential mass irreversibly, making use of equation (18), in the amount of

$$\rho_o{}^2 \pi r^2 \, \Delta E_t \, dr$$

The total energy expended by this process would be

$$E_w = 2\pi\rho_o \int_o^r \Delta E_t r^2 \, dr$$

Since the pressure will remain approximately constant while the projectile is being consumed by shock, this irreversible energy expenditure (waste heat) can be recast into a more convenient form

$$E_w = \frac{2}{3}\pi\rho_o r_o^3 \ \Delta E_{t_i} + 2\pi\rho_o \int_{r_o}^{r} \Delta E_t r^2 \ dr$$

where it is to be understood that r_o is the effective radius of the plug of compressed target material which has been subjected to an increase in the specific internal energy ΔE_{t_i} during the initial partition of energy. An energy balance similar to those in equations (19) and (22) can be written, therefore, as

$$E_a = E_t - E_w \tag{24}$$

with

$$E_a = \frac{2}{3}\pi r^3 \left\{\frac{1}{2} p\eta + \rho_o \left(\frac{a}{b}\right)^2 \left[\frac{b\eta}{1 - b\eta} + \log(1 - b\eta)\right]\right\}$$

$$E_t = \frac{2}{3}\pi r_o^3 p\eta$$

$$\eta = \frac{1}{2}\frac{\rho_o}{p}\left[\frac{2p}{b\rho_o} + \left(\frac{a}{b}\right)^2 - \left(\frac{a}{b}\right)\sqrt{\left(\frac{a}{b}\right)^2 + \frac{4p}{b\rho_o}}\right]$$

Here the energy available for doing useful work in furthering the propagation of the shock through the target has been equated to the difference between the total energy input and the energy lost by irreversible heating.

An explicit solution of equation (24), an integral equation, cannot be obtained for the variation of pressure with radial distance. A numerical solution has been obtained,[3] however, and the results are shown in figure 5, together with the previously discussed $p = p(r)$ variations. With an eye to what follows, the pressure p is presented in all three cases in terms of the dimensionless parameter r/r_o where r_o is, as previously indicated, the effective radius of the compressed target mass at the end of the initial partition of energy.

As expected, the pressure decays more rapidly when consideration is given to the energy deposited irreversibly in the target. At the initial shock pressure of 750 kbars, the pressure varies approximately with $r^{-3.6}$

---

[3]The authors are indebted to Paul F. Byrd of the NASA Ames Research Center for this solution.

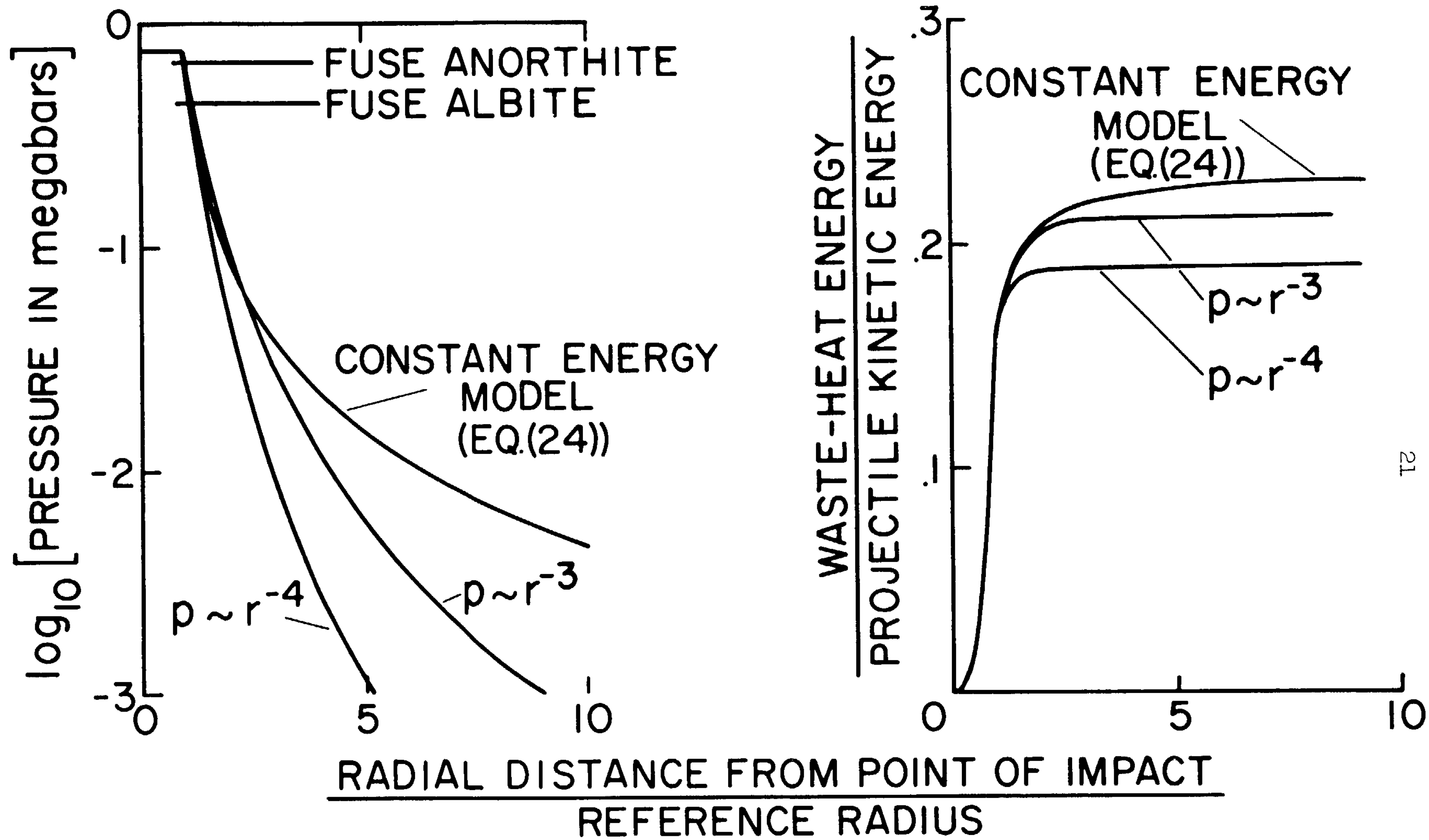

Figure 5.- The radial pressure decay and waste heat in basalt target.

NATIONAL AERONAUTICS AND SPACE ADMINISTRATION
AMES RESEARCH CENTER, MOFFETT FIELD, CALIFORNIA

with waste heat removed from the system (eq. (14)) while the neglect of the waste heat (eq. (12)) yields an $r^{-2.6}$ variation. By the time the pressure has decayed to 100 kbars, these variations have become, respectively, $r^{-2.6}$ and $r^{-2.0}$. At still lower pressures, both calculated results tend toward the $r^{-1.5}$ variation.

It should be pointed out that at pressures lower than about 100 kbars, a multiple wave structure probably occurs in the basalt as a result of material rigidity and the possibility of phase changes in the constituent minerals. In the spirit of the present analysis, however, the presence of multiple waves can be neglected; the computed pressures should be approximately equal to the total pressure jump across one or more waves and the existence of multiple waves would not alter the significant result that waste heat deposited in the target acts to accelerate the decay of pressure with distance from the point of impact.

To estimate the irreversible heating in the basalt target, it should be remembered that, subsequent to the initial penetration of the projectile into the target, rarefaction waves will eat in from the free surface of the interior of the embryonic crater. These waves will attenuate the strength of the shock front even more rapidly than that indicated by equation (24), which is based on a model of cratering which assumes a shell of compressed material with no radial pressure gradients. Since the waste heat decreases with decreasing shock-wave strength, the attenuation of the shock front brought about by the rarefaction waves will reduce the total amount of waste heat which can be deposited in the target as compared to that calculated from equation (24). Thus, although based on a simplified cratering model, equation (24) nevertheless provides a means for estimating the maximum amount of energy deposited irreversibly in the target.

The numerical results calculated for the waste heat from equation (24) are shown in figure 5 normalized with respect to the projectile kinetic energy. For purposes of illustrating the potential attenuating influence of rarefaction waves, results are also presented for two special cases for which $p \sim r^{-3}$ and $p \sim r^{-4}$. It is to be noted that whereas equation (24) corresponds to a conservative system, the two exponential pressure variations represent systems in which the total energy content decreases as the shock front propagates radially outward.

The comparison shown in figure 5 is significant to the present analysis from three considerations. First, it is apparent that the steeper the radial pressure gradient, the less energy is lost irreversibly, as pointed out in a previous paragraph. Second, the major fraction of the irreversible heating occurs during the initial partition of energy (16 percent of the projectile kinetic energy for $r/r_o \lesssim 1.0$) and most of the remaining fraction occurs within a short distance of the original point of impact ($1.0 \lesssim r/r_o \lesssim 2$). Finally, the total amount of energy lost to waste heat is relatively insensitive to the choice of radial pressure gradients, varying from a maximum of 23 percent of the projectile kinetic energy for equation (24) to a minimum of 19 percent of the projectile kinetic energy for $p \sim r^{-4}$. For the present analysis, a range of 19 to 23 percent will be adopted, therefore, for the energy lost to irreversible heating in the target.

The peak specific irreversible heating, amounting to 56 percent of the increase in specific internal energy, is 3×10^{10} ergs/g. This is more than adequate to fuse the mineral constituents of the basalt. Two of these minerals, for example, anorthite and albite, require approximately 1.7×10^{10} and 1.2×10^{10} ergs/g for fusion, respectively. The energy in excess of that required for fusion is insufficient, however, to vaporize these target materials.

Because the specific irreversible heating decreases rapidly with decreasing shock pressures, the radial limits for fusion in the target are attained very quickly as the shock strength decays with radial distance. Figure 6 suggests that the limit of fusion is reached when r/r_o has a value of about 1.10. From the cube of this value (the ratio of the mass of fused target material to the mass of target material engulfed by shock at the termination of the initial partition of energy) multiplied by the ratio of 2.44d/2.75d (see eq. (1)), it is estimated that approximately one projectile mass of target material was fused by the impact. Evidence for this melting in the form of submicron spherules, as mentioned previously, was found in the ejecta recovered from the impacts.

Comminution Energy

Although the strength of the shock wave propagating from the point of impact decays rapidly below the level commensurate with the deposition of a significant amount of irreversible heat energy, the pressure behind the shock front nevertheless persists at a high level relative to the strength of the basalt for a considerable distance into the target. Ultimately, of course, the shock wave decays into elastic waves traveling at the appropriate acoustic velocities for the material, but not before an appreciable mass is subjected to stresses of sufficient magnitude to completely fragment and crush the basalt into fine debris. The energy expended for the comminution of the target medium consumes an important fraction of the projectile kinetic energy.

Before undertaking the calculation of the energy requirements for crushing the basalt, however, it is interesting to note that it is possible to make a reasonable estimate of the mass of material which is crushed as the result of the impact. The compressive strength (unconfined) of the basalt has been determined by conventional static tests to be between 2 and 3 kbars. Grine and Fowles (ref. 18) have indicated that the dynamic strengths of rocks are usually several times greater than static strengths and may be as much as an order of magnitude greater than the static strength. On this basis, therefore, adopting a mean value of 2.5 kbars for the static compressive strength, the dynamic compression strength for the macroscopically homogeneous basalt employed for these studies would be expected to be between 8 and 25 kbars. For the calculated pressure variation with radial distance shown in figure 5, these pressures are attained for values of r/r_o between 3.7 and 7. Since r_o is approximately equal to the radius of the projectile and the projectile and target densities are also approximately equal, it would be expected that a mass of basalt between 50 (the cube of 3.7) and 350 times the mass of the projectile would be crushed by the impact.

Now it has been found, from the experiments, that a total of approximately 370 projectile masses of debris are ejected from the craters for impacts at 6.25 km/sec. Most of this ejected mass consists of large spall plates which occur as the result of shear and tensile failures by the action of rarefaction waves eating in from the free surface of the target face. Between 1/3 to 1/4 of the ejected mass, however, is composed of particles finer than 1 mm, and an approximately equal mass of crushed material forms a lens of fragments at the bottom of the crater. Experimentally, therefore, a mass of crushed fragments of the order of 200 times the projectile mass was produced by the impacts in satisfactory agreement with the estimates based on consideration of the dynamic strength and the pressure decay shown in figure 5. It is to be noted that the use of a target strength of 2.5 kbars, the static value, leads to an unrealistic estimate of 3,000 projectile masses crushed by the impact.

The energy expended for fracturing and crushing the basalt target material will be calculated by two methods. The first and probably the most satisfactory method is based on calculations of the new surface area of the fragmented material. Experimentally determined cumulative mass-size distributions of the fragmented material reported by Gault, et al. (ref. 6) have shown that a simple comminution law

$$\frac{m}{M_e} = \left(\frac{l}{L}\right)^{\alpha} \tag{25}$$

can be used to describe the size distribution of the basalt fragments. Here m is the cumulative (integrated) mass of fragments with a size equal to or smaller than l, M_e is the total mass ejected from the crater, L is the size of the largest fragment, and α is a constant. This expression has been shown to be valid (ref. 6) over a size range 40 microns $< l < L$ with values of $0.3 < \alpha < 0.6$. For fragments smaller than 40μ, the exponent α gradually increases as l approaches what seems to be a cutoff at a minimum size lm. The cutoff for the present experiments appears to be about 0.1 micron.

To calculate the new surface area, A, created by the fragmentation of the target basalt, a modified form of equation (25) is introduced.

$$\frac{m}{M_e} = \left(\frac{l - lm}{L}\right)^{\alpha} \tag{26}$$

where it is to be understood that $l m \ll L$, so that when $l = L$

$$\frac{m}{M_e} = \left(\frac{L - lm}{L}\right)^{\alpha} \approx 1$$

Taking the derivative of equation (26) one obtains the differential mass of fragments dm with fragment sizes between l and $l + dl$

$$dm = \alpha M_e L^{-\alpha}(l - lm)^{\alpha-1}\, dl \tag{27}$$

Then, when dN is defined as the number of fragments with sizes between l and $l + dl$ there results

$$dm = (Km\rho l^3)dN \tag{28}$$

with Km a constant that depends on the geometry of the fragments. Similarly, when dA is defined as the surface area of the dN number of fragments,

$$dA = (Ka l^2)dN \tag{29}$$

with Ka another geometrical constant. Combining these last three equations, the new surface area A can be expressed

$$A = \left(\frac{Ka}{Km}\,\frac{\alpha M_e}{\rho L^{\alpha}}\right) \int_{lm}^{L} \frac{(l - lm)^{\alpha-1}}{l}\, dl \tag{30}$$

A solution for A in explicit form can be obtained only for certain values of α. For the present analysis, a conservative value of $\alpha = 1/2$ is appropriate and leads to

$$A = \frac{\pi}{2}\,\frac{Ka}{Km}\,\frac{M_e}{\rho L}\left(\frac{L}{lm}\right)^{1/2} \tag{31}$$

To evaluate equation (31) numerically, it will be noted that Ka/Km has a value of 6 for spherical and cubic particles. For rectangular or approximately equidimensional blocks or plates representative of the finer fragments which contribute most of the area, values of 5 to 7 for Ka/Km are appropriate. A value of 6, therefore, will be adopted herein.

The mass M_e for the present case of Al into basalt at 6.25 km/sec is approximately 17 g; L can be taken (ref. 6) as 1.7 cm, and $\rho_o = 2.86$ g/cm^3. With a cutoff size $lm = 10^{-5}$ cm, the surface area of the ejecta produced by the impacts becomes

$$A = 1.4 \times 10^4 \text{ cm}^2$$

More than 90 percent of this area is contributed by particles finer than 2×10^{-3} cm. Since the grain size[4] of the minerals in the basalt is almost exclusively between 2×10^{-2} cm and 2×10^{-3} cm, the area is produced by the fragmentation of individual mineral grains, chiefly plagioclase feldspar and augite.

Morrison and Allen (ref. 19) have found that 5.9×10^4 ergs/cm^2 were required to crush a limestone sand by impact at velocities from 0.81 to 0.95 km/sec. Remarkably similar results have been reported by Zeleny and Piret (ref. 20) for drop weight crushing of multiple quartz grains, 7.3×10^4 ergs/cm^2. Although there are differences in loading rates and specific energies between the two sets of data, the lower value for the limestone might be expected, since calcite, the principal constituent of a limestone, has well-defined cleavage planes which should tend to reduce its work input per unit area requirements relative to quartz. Plagioclase feldspar and augite are similar to calcite in this respect. Since they comprise[5] approximately 85 percent by both mass and volume of the basalt, it would seem that the data of Morrison and Allen are probably the most applicable to the present analysis. In view of the uncertainties, however, a mean value of 6.6×10^4 ergs/cm^2 will be adopted for estimating the energy required for fracturing and crushing.

With a new surface area of 1.4×10^4 cm^2, the energy expenditure becomes 9.2×10^8 ergs for the ejected mass of 17 grams. The projectile kinetic energy is 9×10^9 ergs, so that approximately 10 percent of the kinetic energy reservoir was extracted for the comminution of the ejecta.

The impacts break up considerably more mass than the fragments thrown out of the crater. The bottom of the crater, as previously mentioned, consists of a lens of finely crushed and packed debris. In addition, there is an extensive series of radial concentric fractures within and beyond the geometric limits of the cavity, as described by Moore, et al. (ref. 5) at the 5th Hypervelocity Impact Symposium. The surface area and mass of material involved cannot be estimated with any great accuracy but certainly these quantities do not exceed those for the ejected material. On this basis it is believed that the total energy for fracturing and crushing the basalt is greater than 10 percent but could not exceed 20 percent of the projectile kinetic energy.

The percentage values for the comminution energy for the basalt are smaller than the 33 to 40 percent quoted by Morrison and Allen (ref. 19) for the impacts in the limestone sand. The difference is probably attributable to the difference in the impact velocities. In marked contrast to Morrison and Allen's low-speed impact results, 19 to 23 percent of the projectile kinetic energy is lost via irreversible heating of the basalt.

---

[4]Based on petrographic examination by Henry J. Moore, U. S. Geol. Survey, Menlo Park, Calif.

[5]Ibid.

Most of this fraction of energy trapped as heat in the basalt would, at lower impact velocities, become available for fracturing and crushing. For this reason, the sum of comminution energy and irreversible heat energy in the target basalt, 29 to 43 percent, is a more valid basis for comparison with Morrison and Allen's results for low-speed impact.

As an alternative method for estimating the comminution energy, it is interesting to note that Innes (ref. 2), on the basis of results from nuclear explosion experiments, adopts a value of 6.4×10^7 ergs/g to calculate the energy requirements for the formation of large terrestrial meteorite craters. Innes also indicates that (in a personal communication) MacPhail has estimated 6.5×10^7 ergs/g from a study of the debris at the Arizona meteor crater. For purposes of comparison, the present analysis yields a value of 5.4×10^7 ergs/g for the material ejected from the craters in basalt. The three values, obtained by three different methods of analysis, are in surprisingly close agreement and lend support for the belief that a value of 6×10^6 ergs/g suggested by Opik (ref. 21) is unrealistically low.

Application of the values quoted by Innes gives a crushing energy from 12 to 24 percent of the original projectile energy. The 20-percent increase over the values obtained from the work input-free surface area calculations is hardly significant in view of the approximations and generalizations incorporated in the analysis. In the spirit of the analysis, however, a summarizing estimate for the comminution energy will be taken as 10 to 24 percent of the original projectile kinetic energy.

Ejecta Kinetic Energy

The analysis to this point has considered only the energy expended in altering the physical properties and state of target and projectile materials. The formation of the actual crater implies an additional energy expenditure for transporting material away from the point of impact. This energy expenditure associated with the excavation of the crater appears in kinetic form in the fragmented material set in motion by the combined effects of the shock compression and subsequent expansion. As will be shown, a major fraction of the projectile kinetic energy is consumed by this process.

In a previous report Gault, et al. (ref. 6) have presented estimates for the mass-velocity distribution and ejection angle-velocity distribution of the ejecta produced by the impacts in basalt. These data, reproduced herein as figures 6 and 7, respectively, were derived from a series of high-speed framing camera records (nominal 10^4, 10^5, and 10^6 frames/sec) of the impact events. The material ejected with the highest velocity, approximately three times the impact velocity, is believed to be the result of a jetting phenomenon (refs. 22 - 24) which ejects material from between the projectile-target interface during the earliest stages of the initial shock compression of the two media. The jetted material is ejected at

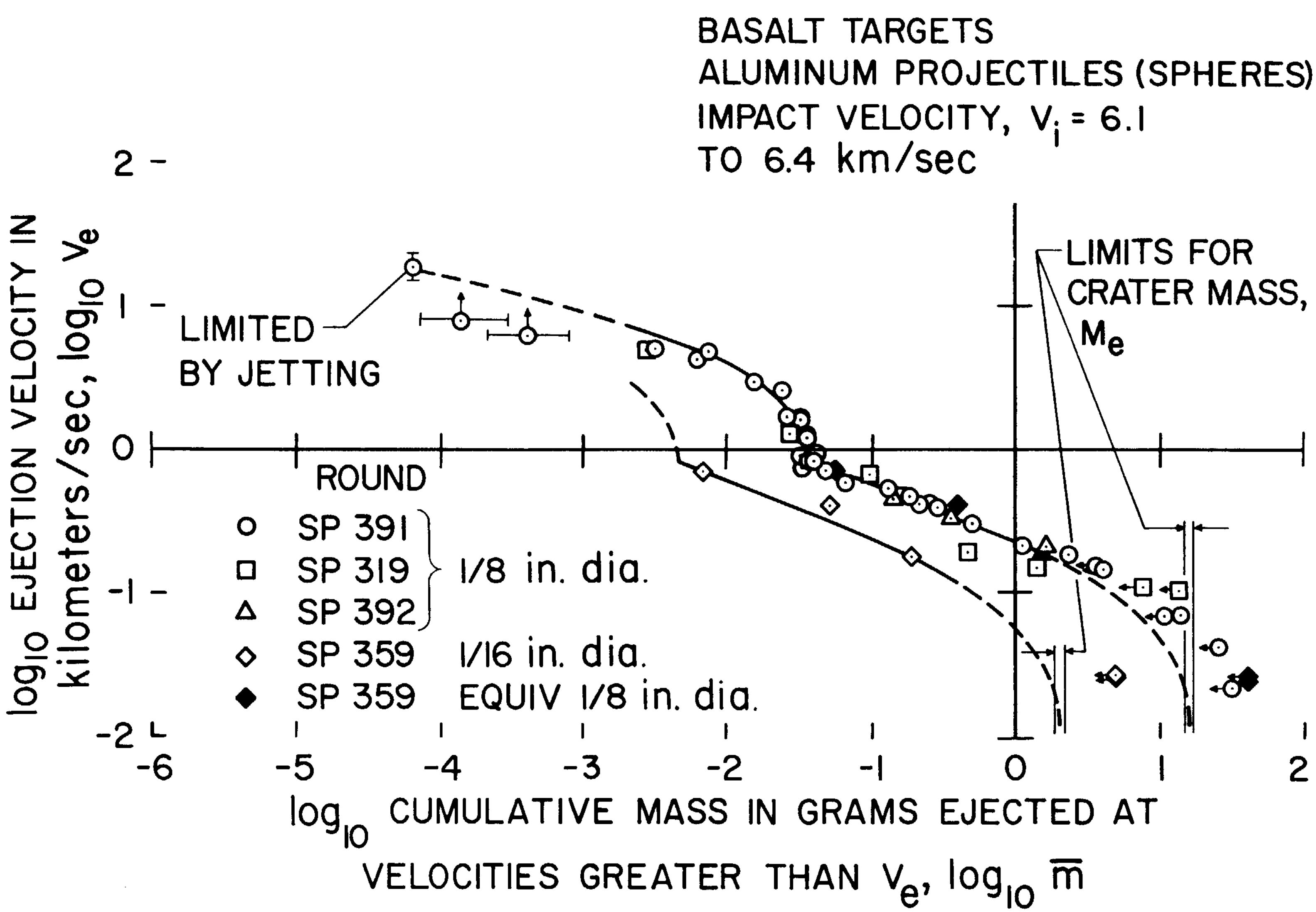

Figure 6.- Cumulative mass-velocity distributions for the ejecta from the craters formed in basalt.

NATIONAL AERONAUTICS AND SPACE ADMINISTRATION
AMES RESEARCH CENTER, MOFFETT FIELD, CALIFORNIA

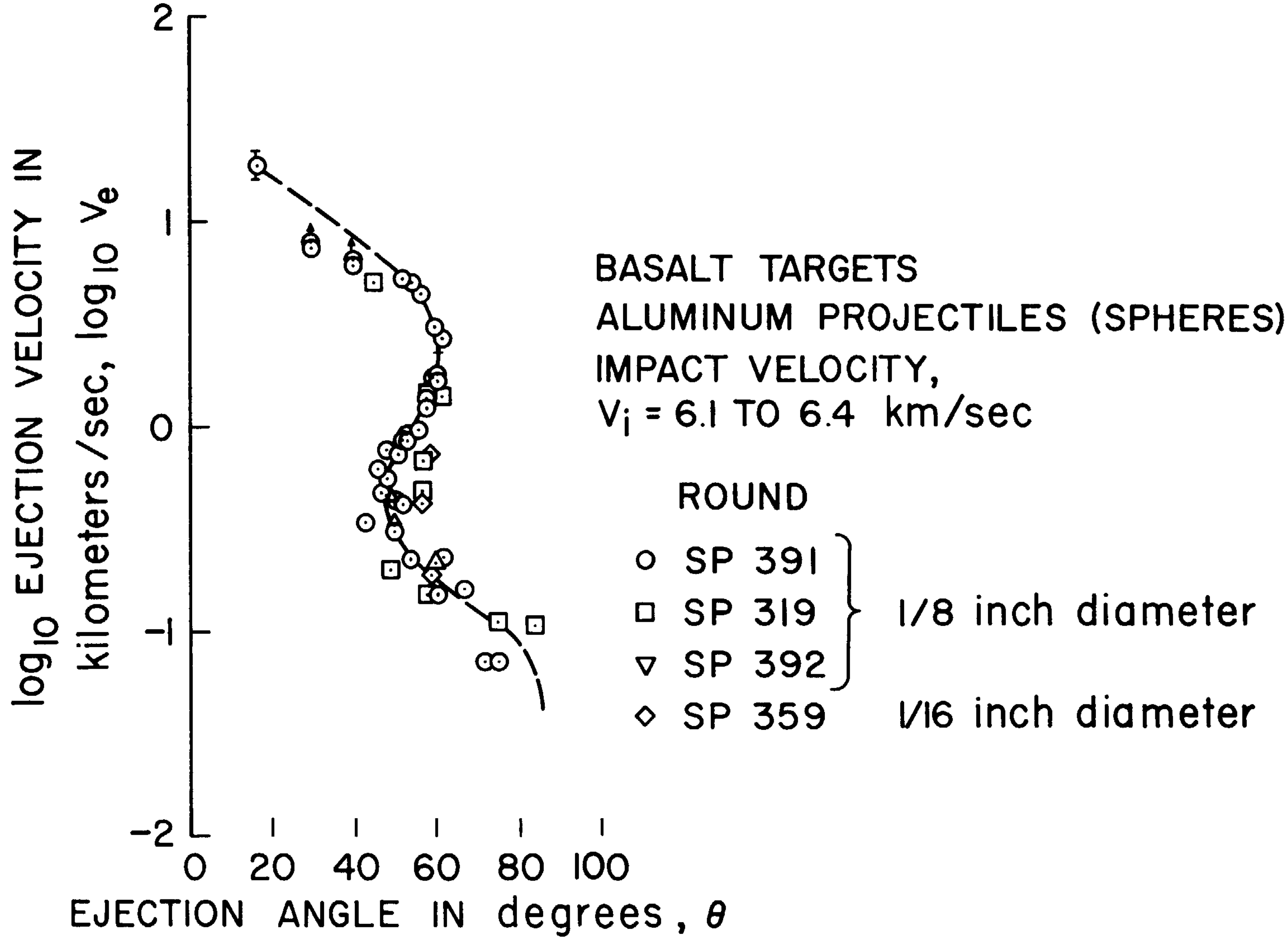

Figure 7.- Ejection angle-velocity distribution for the ejecta from craters formed in basalt.

relatively low angles ($\theta < 30^{\circ}$) relative to the target face and probably consists of fused matter produced by the impact. During the subsequent stages of ejection, the velocity decays rapidly and the ejection angle increases to $\theta = 60^{\circ}$, decreases to about 50°, and finally tends toward 90° as the major fraction of the ejected mass leaves the crater in progressively increasing fragment sizes. The discontinuous variation in the mass-velocity distribution appears to correlate with shock pressures which are consistent with the probable dynamic compressive strength of the basalt. For this reason, the discontinuity is believed to be associated with a transition from plastic to elastic flow behind the shock front as it propagates radially outward from the point of impact.

It is to be noted that figure 6 presents the cumulative mass $\overline{m}$ of material ejected with velocities in excess of a given value of velocity V_e. In functional form one can write

$$\overline{m} = f(V_e) \tag{32}$$

so that

$$d\overline{m} = \frac{d}{dV_e}[f(V_e)]dV_e$$

where $d\overline{m}$ is the differential mass of material ejected with velocities between V_e and $V_e + dV_e$. In this manner, the kinetic energy of the differential mass $d\overline{m}$ can be written

$$\frac{1}{2}\frac{d}{dV_e}[f(V_e)]V_e^2\ dV_e$$

and the total kinetic energy contained in the mass ejected from the crater becomes

$$\frac{1}{2}\int_{V_{e_{max}}}^{o} V_e^2\frac{d}{dV_e}[f(V_e)]dV_e \tag{33}$$

Similarly if the ejection angle θ is expressed as

$$\theta = g(V_e)$$

the component of ejection momentum, acting normal to the target face would be

$$\int_{V_{e_{max}}}^{o} V_e\frac{d}{dV_e}[f(V_e)]\ \sin\ [g(V_e)]dV_e \tag{34}$$

The results obtained from a numerical integration of equations (33) and (34) using the data presented as figures 6 and 7 are shown as figure 8 in normalized form with respect to projectile values. Both the kinetic energy and the momentum are shown in terms of cumulative or integrated quantities measured from the initial mass of material jetted outward by the impact.

The numerical results indicate that 48 percent of the projectile kinetic energy is retained in kinetic form by the ejecta. Most of this energy, approximately 35 percent, is contributed by material spewed out at velocities greater than 1 km/sec. Since the fairing of the experimental data is somewhat arbitrary over the upper range of ejection velocities, several different fairings were evaluated and found to yield values for the kinetic energy content in the ejecta differing by approximately ±5 percent of the projectile kinetic energy. On this basis, therefore, the kinetic energy for the ejected mass from the craters in basalt is taken to be from 43 to 53 percent of the projectile kinetic energy.

It is interesting to note that although not specifically concerned with the energy partition for the impacts in basalt, the calculated total momentum of the ejecta is in satisfactory agreement with results from ballistic pendulum measurements of the momentum imparted to the target blocks. In contrast to the kinetic energy, most of the momentum in the ejecta is provided by material traveling at velocities less than 1 km/sec. The scatter in the ballistic pendulum data is attributable to erratic spalling of the largest fragments thrown out of the craters. The mass of the largest fragments is between one to two orders of magnitude greater than the projectile mass while the ejection velocity is from one to two orders of magnitude less than the impact velocity. The combined effect of erratic mass and ejection velocity for large fragments, therefore, can readily produce large fluctuations in the momentum sensed by the pendulum.

Elastic Wave and Radiant Energy

Although the strong shock wave produced in the target by the impact ultimately decays into elastic waves which cause no permanent damage to the target material, the energy contained in the waves has not been considered in the preceding analysis. Evidence of such waves is demonstrated by the spallation fractures observed in the back of all the target blocks, as illustrated by figure 9. As for most rocks, the tensile strength (100 to 200 bars) of the basalt is much lower than the compressive strength (2 to 3 kbars). For this reason, any elastic compressive disturbance when reflected from the free surface of the basalt as a tension wave would produce tensile failures even though the peak compressive stresses are inadequate to produce compressive failures.

A thorough discussion of wave reflection from a free surface has been given by Rinehart (ref. 17) and will be omitted here. It is sufficient to note that the spallation at the back of the target, shown in figure 9,

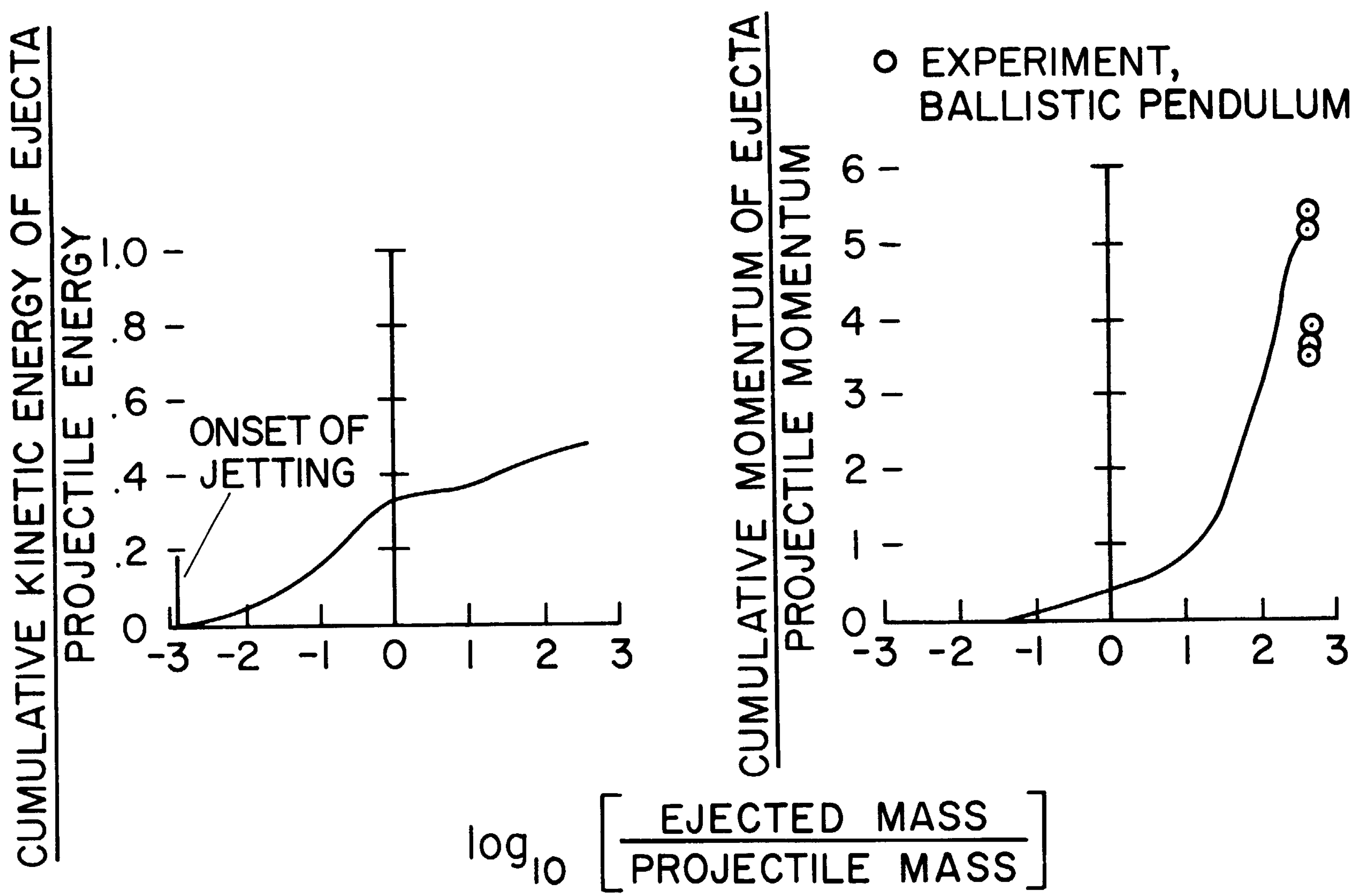

Figure 8.- Cumulative kinetic energy and cumulative momentum of the ejecta from the craters formed in basalt.

Figure 9.- Photograph of sectioned crater in basalt showing spall fractures at the back of the target block.

NATIONAL AERONAUTICS AND SPACE ADMINISTRATION
AMES RESEARCH CENTER, MOFFETT FIELD, CALIFORNIA

indicates three spalls were produced by the impact. With a tensile strength of 200 bars, the peak stress in an incident elastic compressive wave must have been at least 600 bars and perhaps approached 800 bars. Since the distance from the free surface to the last spallation surface is 1.2 cm, the length of the compressive wave was probably between 1.2 and 1.6 cm. If the stress distribution along the wave is assumed to decrease linearly from the peak value (triangular wave shape) and the particle velocity for the peak stress is estimated by means of equation (3a) (using a density of 2.86 g/cm^3, and the acoustic velocity of 5.5 km/sec), the total energy content of the elastic wave (taken to have a hemispherical geometry) could not exceed 1 percent of the original projectile kinetic energy.

One final method for expending energy deserves mention, the production of radiant energy associated with impact flash commonly observed in the laboratory. Results described by MacCormack (ref. 24) for the impact of Al into Al at a nominal 2.5 km/sec give a value for the total radiant energy of the order of 10^{-4} percent of the projectile kinetic energy. Although this result is based on conditions which differ in materials and impact velocity from those of the present study, the result suggests that the contribution of radiant energy for present purposes can be safely ignored. This is particularly true if the radiant energy represents a conversion of ejecta kinetic energy to light as concluded by MacCormack; consideration has been given to the ejecta kinetic energy, and the subsequent conversion or expenditure of the ejecta energy to radiant energy would be redundant for the present analysis.

CONCLUDING REMARKS

The results from the analysis of the partition of energy for the impact of aluminum into basalt are summarized in the following tabulation:

Energy expended for:	Percentage of projectile kinetic energy
(1) Irreversible and waste heat	
Projectile	4 to 12
Target	19 to 23
(2) Comminution	10 to 24
(3) Ejecta throwout	43 to 53
(4) Miscellaneous	
Residual elastic wave	less than 1
Radiant	negligible
Total:	77 to 113

The final results in terms of an energy balance indicate that the analysis has accounted for the expenditure of 95 ±18 percent of the original projectile kinetic energy. This balance is, perhaps, entirely satisfactory in view of the uncertainties and approximations introduced during the analysis. It is believed, however, the results are somewhat better than one might judge from just a superficial examination of the tabulation. The minimum values in the table for both the comminution energy and projectile irreversible heat are unrealistically low. Better minimum value estimates would be 14 to 16 and 8 to 10 percent, respectively. With these new values, the final balance would become 100 ±12 or 13 percent. This latter balance is believed to provide a more representative quantitative interpretation of the results.

It is interesting to note that the maximum energy expenditure required for removing material from the crater is less than 10^{-5} percent of the original projectile kinetic energy. Approximately one-half of the original reservoir of projectile energy, therefore, was wasted by ejection of debris with velocities far in excess of those required to move material beyond the geometric limits of the final crater. In addition, approximately 30 percent of the projectile kinetic energy was wasted as heat in the target and projectile. Of the remaining 20 percent of the available projectile energy, only about 10 percent can be considered to have been spent usefully in crushing the target material actually removed from the crater. Excavation of a crater by hypervelocity impact would appear to be an extremely inefficient process.

Although an estimated 30 percent of the projectile kinetic energy was expended as heat in target and projectile material, most of this heat energy was utilized for fusion and, perhaps, on the basis of a tenuous assumption, some vaporization of the projectile. The analysis and calculated results, however, clearly provide no supporting evidence for perpetrating the concept of "explosive" cratering. The craters formed in basalt occurred as the result of fracturing and crushing the target material by a mechanical shock compression followed by an ejection of the fragmented debris by the action of rarefaction waves.

Finally, attention is drawn to the fact that for higher impact velocities, the percentage of the projectile kinetic energy lost by irreversible heating will increase at the expense of the energy available for fragmentation and ejection of target material. Since higher impact velocities imply higher ejection velocities, the relative increase in irreversible heat would be at the expense of fragmentation. With constant energy input, therefore, total ejected mass and crater dimensions should decrease as the impact velocity increases. This interpretation suggests that one cannot expect a direct mass (or volume) proportionality with projectile energy throughout a wide range of impact velocities.

REFERENCES

1. Shoemaker, Eugene M.: Impact Mechanics at Meteor Crater, Arizona. Open File Report, U. S. Geological Survey, Menlo Park, Calif., 1959.

2. Innes, M. J. S.: Gravity of Meteorite Craters. Jour. Geo. Res., vol. 66, no. 7, 1961, pp. 2225-2239.

3. Shoemaker, E. M., and Chow, E. C. T.: Impact Origin of the Ries Basin, Bavaria, Germany. Jour. Geo. Res., vol. 66, 1961, pp. 3371-3378.

4. Dietz, Robert S.: Vredefort Ring Structure: Meteorite Impact Scar? Jour. of Geol., vol. 69, Sept. 1961, pp. 499-516.

5. Moore, H. J., Gault, D. E., and Lugn, R. V.: Experimental Hyper-velocity Impact Craters. Proc. 5th Symposium on Hypervelocity Impact, vol. I, pt. 2, April 1962, pp. 625-643.

6. Gault, Donald E., Shoemaker, Eugene M., and Moore, Henry J.: Spray Ejected From the Lunar Surface by Meteoroid Impact. NASA TN D-1767, 1963.

7. McQueen, R. G., and Marsh, S. P.: Equation of State for Nineteen Metallic Elements from Shock-Wave Measurements to Two Megabars. Jour. of Appl. Phys., vol. 31, no. 7, July 1960, pp. 1253-1269.

8. Walsh, John M., Rice, Melvin H., McQueen, Robert G., and Yarger, Frederick L.: Shock Wave Compressions of Twenty-Seven Metals. Equations of State Metals. Phys. Rev., vol. 108, no. 2, Oct. 1957, pp. 196-216.

9. Al'tshuler, L. V., Kormer, S. B., Bakanova, A. A., and Trunin, R. F.: Equation of State for Aluminum, Copper and Lead in the High Pressure Region. Soviet Physics JETP, vol. 11, no. 3, Sept. 1960, pp. 573-579.

10. Al'tshuler, L. V., Bakanova, A. A., and Trunin, R. F.: Shock Adiabats and Zero Isotherms of Seven Metals at High Pressures. Soviet Physics JETP, vol. 15, no. 1, July 1961, pp. 65-74.

11. Lombard, David B.: The Hugoniot Equation of State of Rocks. UCRL-6311, University of California, Lawrence Radiation Laboratory, Feb. 1961.

12. Rice, M. H., McQueen, R. G., and Walsh, J. M.: Compression of Solids by Strong Shock Waves. Solid State Physics, vol. 6, Academic Press, 1958, pp. 1-63.

13. Charters, A. C.: High Speed Impact. Scientific American, vol. 203, 1960, pp. 128-140.

14. Moore, H. J., Gault, D. E., Lugn, R. B., and Shoemaker, E. M.: Hypervelocity Impact of Steel into Coconino Sandstone. Proc. Geophysical Laboratory - Lawrence Radiation Laboratory Cratering Symposium. UCRL-6438, Paper N, pt. II, Oct. 1961.

15. Porzel, F. B.: Close-in Shock Time-of-Arrival Measurements and Hydrodynamical Yield. Proc. Second Plowshare Symposium, UCRL-5674, pt. I, 1959, pp. 28-49.

16. Charters, A. C., and Summers, James L.: Comments on the Phenomena of High-Speed Impact. NOLR 1238, U. S. Naval Ordnance Laboratory, White Oak, Silver Springs, Md., May 25-26, 1959, pp. 200-221.

17. Rinehart, John S.: On Fractures Caused by Explosions and Impacts. Quarterly of the Colorado School of Mines, vol. 55, no. 4, Oct. 1960.

18. Grine, D. R., and Fowles, G. R.: The Attenuation of Shock Waves in Solid Materials with Seismic Applications. Third Symposium on Rock Mechanics, Colorado School of Mines Quarterly, vol. 54, 1959, pp. 251-269.

19. Morrison, H. L., and Allen, W. A.: New Surface Area Formed by a Projectile Striking Limestone Particles. Meteoritics, vol. I, no. 3, 1955, pp. 328-335.

20. Zeleny, Richard A., and Piret, Edgar L.: Studies of the Energy Requirements for Crushing. Third Symposium on Rock Mechanics, Colorado School of Mines Quarterly, vol. 54, 1959, pp. 35-42.

21. Öpik, E. J.: Meteor Impact on Solid Surface. Irish Astronomical Journal, vol. 5, no. 1, March 1958, pp. 14-36.

22. Walsh, J. M., Shreffler, R. B., and Willig, F. J.: Limiting Conditions for Jet Formation in High Velocity Collisions. Jour. Appl. Phys., vol. 24, no. 3, March 1953, pp. 349-359.

23. Birkhoff, Garret, MacDougall, Duncan P., Pugh, Emerson M., and Taylor, Geoffery: Explosives With Lined Cavities. Jour. Appl. Physics, vol. 19, June 1948, pp. 563-582.

24. Allen, William A., Morrison, Harvey L., Ray, Daniel B., and Rogers, James W.: Fluid Mechanics of Copper. The Physics of Fluids, vol. 2, no. 3, May 1959, pp. 324-333.

25. MacCormack, Robert W.: Investigation of Impact Flash at Low Ambient Pressures. Paper presented at the 6th Symposium on Hypervelocity Impact, Cleveland, Ohio, April 30-May 1,2, 1963.